Chemical Science

ROYAL SOCIETY OF CHEMISTRY

EDGE ARTICLE

Cite this: *Chem. Sci.*, 2024, **15**, 7187

All publication charges for this article have been paid for by the Royal Society of Chemistry

Received 4th March 2024
Accepted 9th April 2024

DOI: 10.1039/d4sc01503g

rsc.li/chemical-science

Controlling the regioselectivity of the bromolactonization reaction in HFIP†

Tuong Anh To, ‡[a] Nhu T. A. Phan,‡[a] Binh Khanh Mai *[b] and Thanh Vinh Nguyen *[a]

The halolactonization reaction provides rapid access to densely functionalized lactones from unsaturated carboxylic acids. The *endo*/*exo* regioselectivity of this cyclization reaction is primarily determined by the electronic stabilization of alkene substituents, thus making it inherently dependent on substrate structures. Therefore this method often affords one type of halolactone regioisomer only. Herein, we introduce a simple and efficient method for regioselectivity-switchable bromolactonization reactions mediated by HFIP solvent. Two sets of reaction conditions were developed, each forming *endo*-products or *exo*-products in excellent regioselectivity. A combination of computational and experimental mechanistic studies not only confirmed the crucial role of HFIP, but also revealed the formation of *endo*-products under kinetic control and *exo*-products under thermodynamic control. This study paves the way for future work on the use of perfluorinated solvents to dictate reaction outcomes in organic synthesis.

Introduction

Halonium-promoted addition of nucleophiles to alkenes is one of the most fundamental reactions in organic chemistry, which offers widespread applications in organic synthesis.[1] The intramolecular variant of this transformation is a powerful tool to construct molecular complexity by not only creating a new ring and stereogenic centres but also introducing a halide group for subsequent functionalizations.[2] Halolactonization is a typical example of this transformation, offering rapid access to densely functionalized lactones from acyclic unsaturated carboxylic acids. A wide range of valuable lactone analogues varying in both structures and stereochemistry could be obtained through this protocol by controlling the diastereoselectivity, enatioselectivity, and regioselectivity of the reaction (Scheme 1a).[3] Traditionally, diastereoselective and enantioselective halolactonizations are usually directed by substrate structures.[3a,b] Over the past two decades, there have been also developments of reagent-controlled enantioselective halolactonization, relying on chiral electrophilic halogenating reagents which in turn can be generated *in situ* through the coordination of chiral catalysts to halogenating reagents.[4] On the other hand, regioselectivity of halolactonization has predominantly been dictated by the electronic effects of alkene substituents, with carboxylate groups intercepting halonium intermediates at the position where positive charge stabilization is most favorable. To the best of our knowledge, methods to alter this inherent regioselectivity of halolactonization or offer controllable formation of both regioisomers from one single unsaturated carboxylic acid substrate are scarce in the literature.[5]

In the last decade, hexafluoroisopropanol (HFIP) has attracted increasing attention as a reaction solvent due to its strong hydrogen-bond donating ability, low nucleophilicity, stability under redox conditions and most importantly the unique capacity to stabilize ionic reaction intermediates.[6] HFIP has also demonstrated its ability to facilitate a wide range of difunctionalization reactions.[7] In relevant context to this work, there have been seminal contributions from the Gulder group[8] on HFIP-mediated halocyclization of terpenes, and the Lebœuf and Gandon groups[9] on HFIP-mediated haloamidation and halolactonization of alkenes with excellent reaction outcomes (Scheme 1b). Building upon these research studies and our prior investigations on halide-promoted addition reaction to alkenes,[10] acid-promoted cyclization reactions[11] and HFIP-assisted Brønsted acid-catalyzed chemistry,[12] we envisaged that HFIP can be used to activate bromonium sources such as NBS and promote *endo*-bromolactonization of readily available conjugated unsaturated carboxylic acids[13] (Scheme 1c, upper route). On the other hand, the other bromolactonization regioisomers with smaller ring sizes are inherently more thermodynamically stable but require higher activation energies due to the lack of

[a]*School of Chemistry, University of New South Wales, Sydney, NSW 2052, Australia. E-mail: t.v.nguyen@unsw.edu.au*

[b]*Department of Chemistry, University of Pittsburgh, Pennsylvania 15260, USA. E-mail: binh.mai@pitt.edu*

† Electronic supplementary information (ESI) available: Experimental procedures and methods, characterization data, NMR spectra, computational methods and energies and Cartesian coordinates. See DOI: https://doi.org/10.1039/d4sc01503g

‡ Contributed equally.

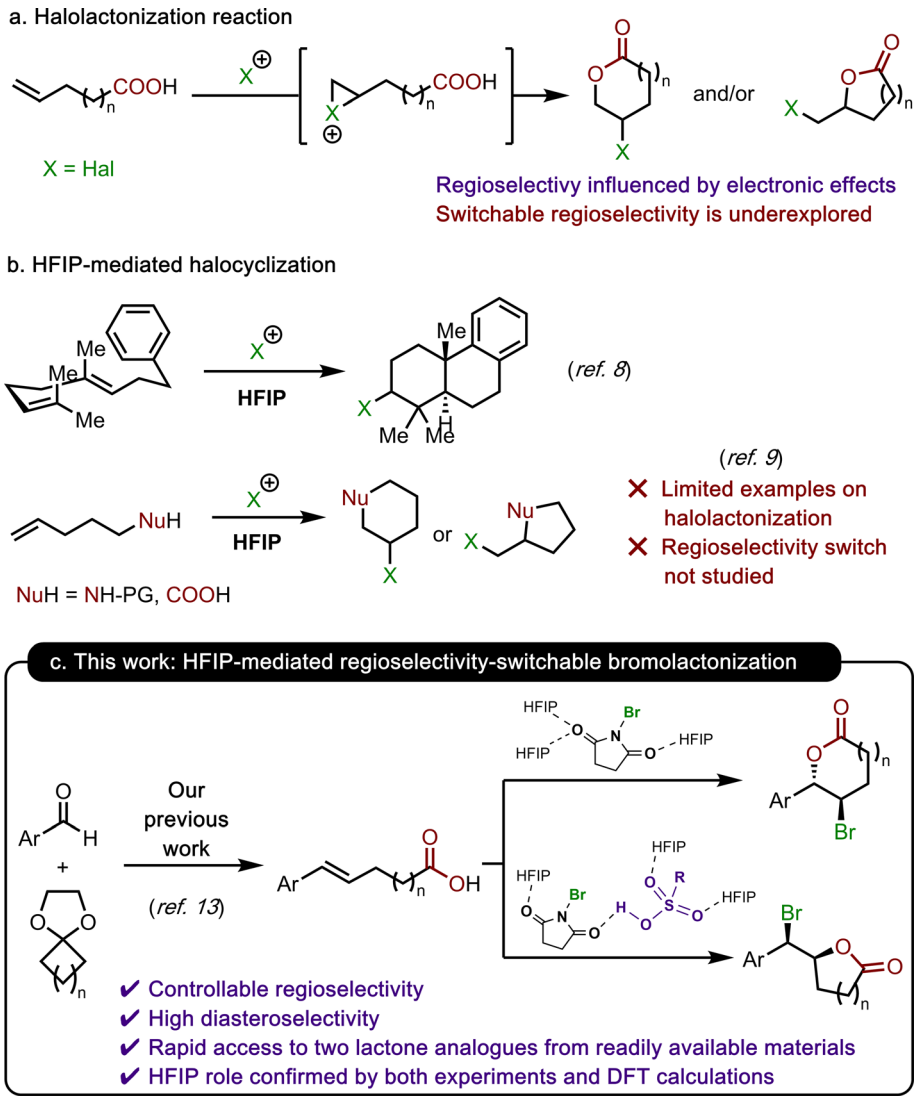

Scheme 1 (a) Halolactonization reaction; (b) HFIP-mediated halocyclization; and (c) this work: HFIP-mediated regioselectivity-switchable bromolactonization.

electronic stabilization from the aromatic ring. We believed that the presence of HFIP-activated Brønsted acid catalysts can potentially activate the reaction substrates to overcome these higher activation energy barriers, leading to the formation of the *exo*-cyclization product (Scheme 1c, lower route). This novel regioselectivity-switchable protocol would enable rapid regioselective synthesis of two different analogues of densely functionalized lactones from readily available precursors.

Results and discussion

We elected to focus on bromolactonization in this work, as brominating reagents and their corresponding products possess balanced reactivity and stability compared to chloro or iodo counterparts. We initiated this study by choosing **1a**, which was efficiently obtained by ring-opening olefination of cyclopentanone ketal according to our recent work,[13] as the model substrate and *N*-bromosuccinimide (NBS) as a brominating reagent, which can generate ε-caprolactone **2a** and δ-valerolactone **3a** as *endo*-cyclization and *exo*-cyclization products respectively (Table 1). The bromolactonization of **1a** in HFIP happened smoothly at room temperature, selectively forming *endo*-product **2a** in 91% yield with a 13/1 regioisomer ratio (entry 1, Table 1). Both reactivity and selectivity of this HFIP-mediated *endo*-bromolactonization are in accordance with Lebœuf and Gandon work.[9] Lowering the reaction temperature to 0 °C, with a slight decrease in yield and longer reaction time, resulted in absolute selectivity to *endo*-product **2a** (entry 2). This observation is in agreement with our initial hypothesis that *endo*-products of bromolactonization reactions are kinetically favorable while *exo*-products are thermodynamically favorable. For a simple reaction setup and better reaction efficiency, we chose to carry out the reaction at room temperature in subsequent studies.

On the other hand, introducing a catalytic amount of Brønsted acids into the reaction, as predicted, shifted the selectivity towards the *exo*-product **3a** while maintaining

Table 1 Optimization of HFIP-mediated regioselectivity-controllable bromolactonization

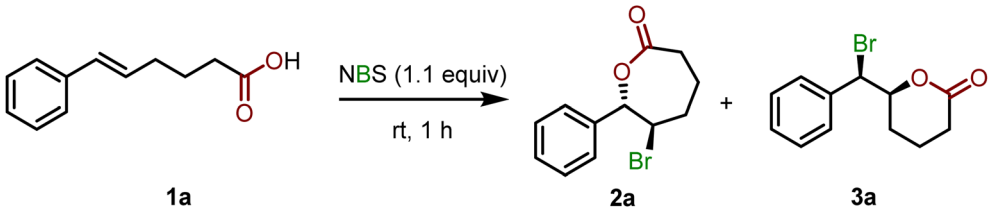

1a 2a 3a

Entry[a]	Catalyst (mol%)	Solvent (v/v)	Yield of 2a[b]	Yield of 3a[b]	2a/3a ratio[b]
1		**HFIP**	**91%**	**7%**	**13/1**
2[c]		HFIP	77%	Traces	>20/1
3	AcOH (10%)	HFIP	88%	10%	8.8/1
4	TFA (10%)	HFIP	67%	20%	3.4/1
5	pTSA (10%)	HFIP	Traces	89%	<1/20
6	TfOH (10%)	HFIP	Traces	86%	<1/20
7	**pTSA (5%)**	**HFIP**	**Traces**	**87%**	**<1/20**
8	pTSA (2%)	HFIP	Traces	79%	<1/20
9		HFIP/DCE (1/1)	85%	8%	10.6/1
10		HFIP/DCE (3/7)	85%	9%	9.4/1
11		HFIP/DCE (1/9)	71%	Traces	>20/1
12		DCE	ND	ND	—
13		TFE	29%	60%	1/2.1
14		iPrOH	ND	ND	—
15		$MeNO_2$	Traces	Traces	—
16	pTSA (5%)	DCE	11%	5%	2.2/1
17	pTSA (5%)	TFE	22%	12%	1.8/1
18	pTSA (5%)	iPrOH	13%	5%	2.6/1
19	pTSA (5%)	$MeNO_2$	17%	20%	1/1.2

[a] Reaction conditions: **1a** (0.1 mmol), NBS (1.1 equiv.), catalyst, and solvent (v/v, 0.1 M) were stirred at room temperature for 1 h. [b] Yields and regioisomer ratios were determined by ^{1}H NMR using methyl benzoate as an internal standard. See pages S4–S5 in the ESI for full optimization studies. ND = not detected. [c] Reaction was carried out at 0 °C for 2 h.

excellent overall yields of both products (Table 1, entries 3–8). Interestingly, weaker acids such as acetic acid (AcOH, entry 2) and trifluoroacetic acid (TFA, entry 4) caused minor shifts in selectivity, whereas stronger acids like *p*-toluenesulfonic acid (pTSA, entry 5) and triflic acid (TfOH, entry 6) induced a complete alteration in selectivity toward *exo*-product **3a**. pTSA was chosen for further studies of *exo*-bromolactonization as it is inexpensive and easier to handle. Reducing the amount of pTSA to 5 mol% did not change the reaction efficiency (entry 7) while the yield of *exo*-product **3a** slightly decreased when employing 2 mol% of pTSA (entry 8). We also attempted to reduce the amount of HFIP in *endo*-bromolactonization by using DCE as a co-solvent, but both yield and selectivity slightly dropped (entries 9–11). To clarify the role of HFIP in this reaction, we carried out the reaction in DCE as a typical solvent for halocyclization chemistry, trifluoroethanol (TFE) as a weaker hydrogen-bonding donor solvent, isopropanol as the respective non-fluorinated alcohol, and nitromethane ($MeNO_2$) as a highly polar solvent for charge stabilization (entries 12–19). Without HFIP as solvent, reactions generally led to unsatisfactory outcomes, regardless of whether or not there was a Brønsted acid catalyst, confirming the crucial role of HFIP in the formation of both *endo*- and *exo*-products.

We subsequently explored the versatility of our newly developed method in both *endo*-bromolactonization (Scheme 2a) and *exo*-bromolactonization (Scheme 2b). A series of unsaturated carboxylic acid **1** were first subjected to our optimal conditions for *endo*-bromolactonization. Substrates with diverse electronic and steric effects (**1a–j**) were well tolerated under *endo*-bromolactonization conditions, yielding 7-*endo*-products **2a–j** in moderate to excellent yields. Electron-rich thiophene substrate **1k** led to poor efficiency, probably due to susceptibility to electrophilic bromination on the electron-rich aromatic ring in HFIP medium.[14] Our method also demonstrated good efficiency in 6-*endo*-bromolactonization, generating 6-*endo*-product **2l** in good yield. However, 8-*endo*-bromolactonization exhibited unimpressive efficiency (products **2m** and **2n**), which can presumably be attributed to the challenging formation of eight-membered medium-sized lactones.

A quite similar trend in reaction yields was also observed when the same set of unsaturated acids **1** was subjected to our optimal conditions of *exo*-bromolactonization (Scheme 2b). In the case of δ,ε-unsaturated carboxylic acids, except for substrates with an electron-rich aromatic ring (**1f** and **1k**), which are sensitive towards electrophilic aromatic bromination,[14,15] other substrates (**1a–e** and **1g–j**) exhibited a complete switch in regioselectivity to 6-*exo*-bromolactonization with moderate to excellent yields when treated with a Brønsted acid catalyst in HFIP. Absolute *exo*-regioselectivity and excellent

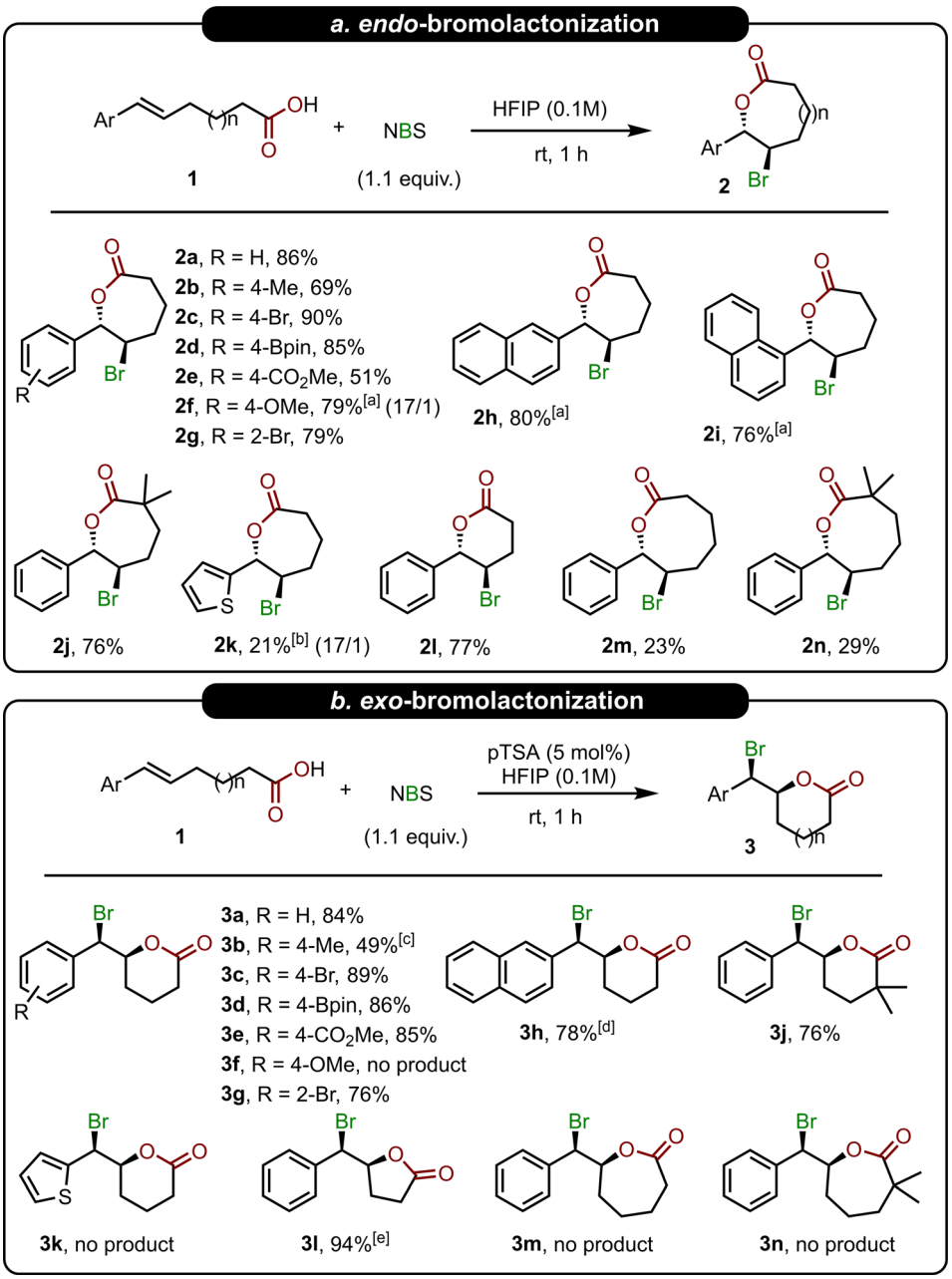

Scheme 2 Substrate scope of (a) *endo*-bromolactonization and (b) *exo*-bromolactonization. Reaction conditions unless otherwise noted: **1** (0.2 mmol), NBS (1.1 equiv.), with/without pTSA (5 mol%), HFIP (0.1 M). Diastereomeric ratios were all >20/1 without quoted ratios in parentheses. [a] HFIP/DCM (1/4, 0.1 M) was used. [b] HFIP/DCM (1/99, 0.1 M) was used. [c] Reaction was stirred without catalyst for 1 h prior to adding catalyst and further stirring for 1 h. [d] NMR yield. [e] TfOH (10 mol%) was used.

yield were also observed with γ,δ-unsaturated carboxylic acid **1l**, while no expected products **3m** and **3n** were detected for the case of ε,ζ-unsaturated carboxylic acids **1m** and **1n**. It should be noted that along with controllable regioselectivity, our method also offered excellent to absolute diastereoselectivity for both *endo*- and *exo*-cyclization.

Next, we extended the substrate scope of HFIP-mediated bromolactonization to other alkenoic acid scaffolds (Scheme 3). Estrone-derived δ,ε-unsaturated carboxylic acid **1o**, obtained by modifying estrone through a three-step procedure as reported in our recent work,[13] smoothly underwent 7-*endo*-bromolactonization, yielding tetracyclic lactone **2o** as an equimolar mixture of two diastereomers in 88% yield. Similar to substrates in Scheme 2b, the regioselectivity completely shifted to 6-*exo*-product **3o**, also as an equimolar mixture of two diastereomers in excellent yield, when a catalytic amount of pTSA was used to promote the reaction (Scheme 3a). This example demonstrated a quick and efficient way for the late-stage modification of complex cyclic ketones into lactones with various ring-sizes.

As discussed earlier in Scheme 2, we believe that the selective formation of *endo*-product **2** is kinetically favored due to

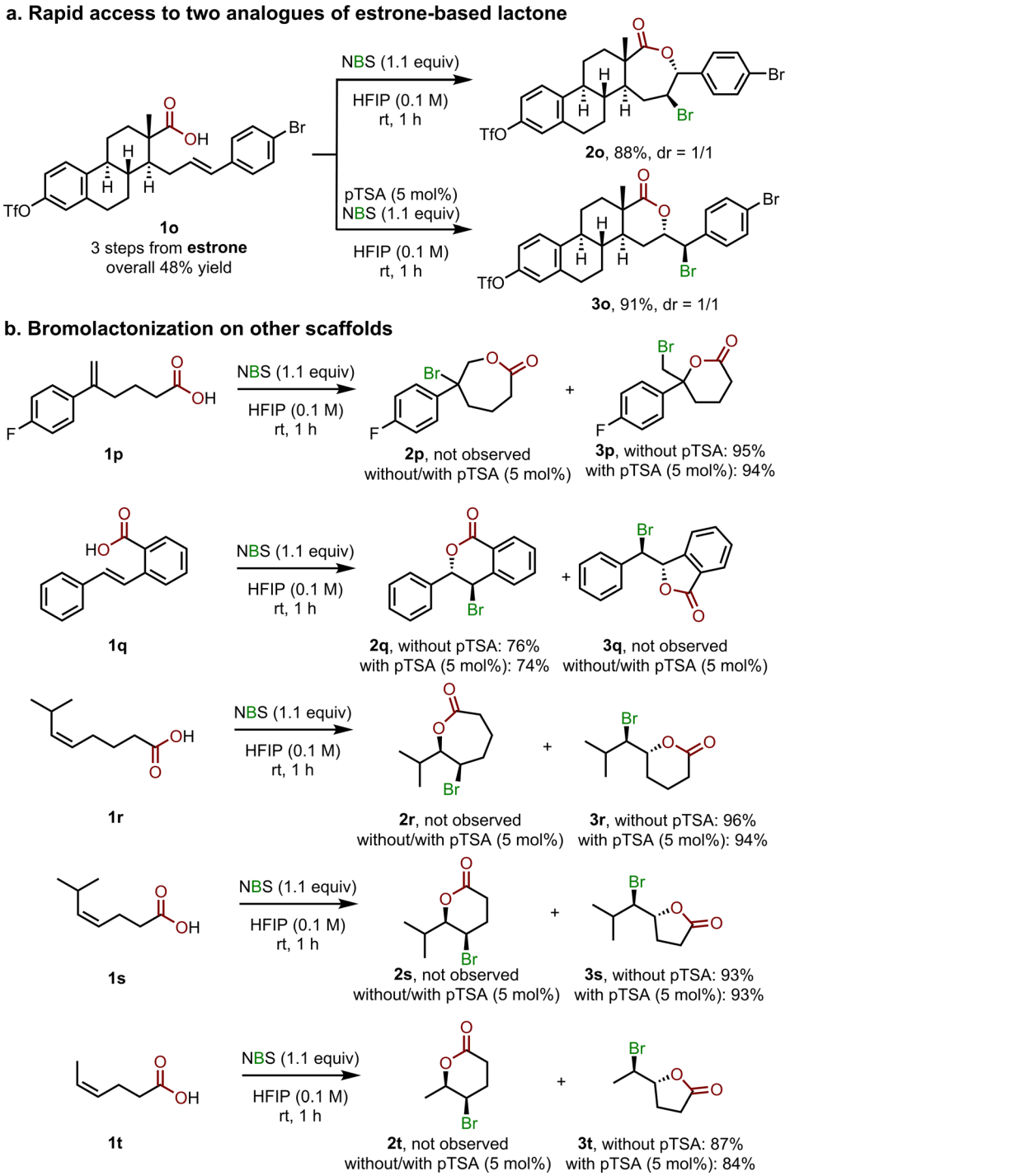

Scheme 3 Expanding the substrate scope of bromolactonization: (a) rapid access to two analogues of estrone-based lactone and (b) bromolactonization on other scaffolds.

benzylic stabilization, and the selective formation of *exo*-product **3** is thermodynamically supported due to generation of a more stable ring size. To support this hypothesis, we carried out some negative testing studies with two other structures often encountered in halolactonization chemistry, terminal alkenoic acid **1p** and *trans*-stilbene-type acid **1q**. Gratifyingly, both of these exclusively yielded *exo*-product **3p** and *endo*-product **2q**, respectively in good to excellent yields, regardless of whether catalytic pTSA was used or not (Scheme 3b). These outcomes align well with our hypothesis, as **3p** and **2q** are both kinetically and thermodynamically favorable, owing to both benzylic stabilization and the formation of a more stable ring size. As a result, this leads to an unswitchable regioselectivity with substrates **1p** and **1q**.

We also attempted to exclude benzylic stabilization by carrying out reactions on aliphatic unsaturated acids **1r–t**,

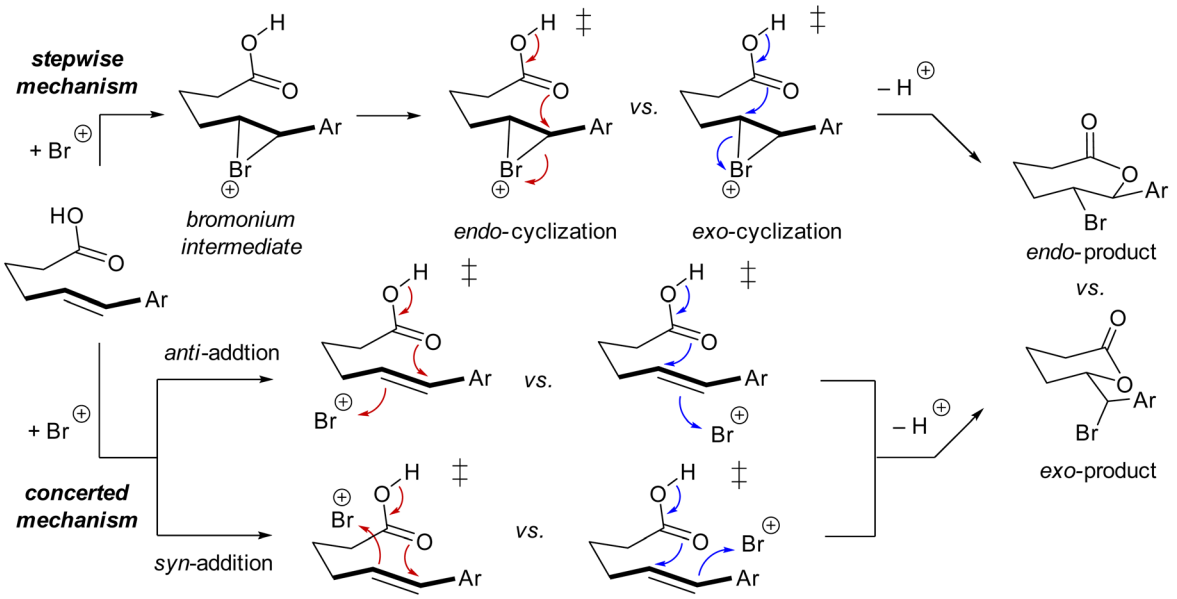

Scheme 4 Proposed reaction mechanism for the bromolactonization.

which have nearly identical electronic effects on both reactive sites. Isopropyl-substituted acids **1r** and **1s** exclusively yielded 6-*exo*-product **3r** and 5-*exo*-product **3s** in excellent yields in the presence or absence of the pTSA catalyst, respectively. Unswitchable regioselectivity and excellent yield were also recorded on a less sterically hindered methyl-substituted acid **1t**. These results confirmed the importance of the benzylic effect on the controllable regioselectivity.

To gain better insights into the reaction mechanism and effect of catalyst/solvent on the regioselectivity for the bromolactonization, we then turn our effort to density functional theory (DFT) calculations at the MN15/6-311+G(2d,2p)/SMD//M06-2X/6-31G(d,p)/SMD level of theory (see page S97 in the ESI† for computational details). The proposed reaction mechanism for the bromolactonization is shown in Scheme 4. Traditionally, this transformation is expected to take place *via* a stepwise Ad_E2-type mechanism. The first step of this reaction is the electrophilic addition of the bromine atom to the C=C double bond of the substrate generating a reactive cyclic bromonium intermediate, which is followed by a nucleophilic addition leading to *endo*- and *exo*-cyclic products.[16] Alternatively, by means of kinetics studies, NMR spectroscopy, and DFT calculations, Jackson and Borhan[17] proposed that the halolactonization can take place *via* a concerted Ad_E3-type mechanism in which the nucleophilic and electrophilic additions happen simultaneously and no ionic intermediate is generated during the reaction. Moreover, the additions of the nucleophile and electrophile can occur at the same face (*i.e.*, *syn*-addition) or opposite faces (*i.e.*, *anti*-addition) of the C=C double bond (Scheme 4).[17]

We first performed DFT calculations to elucidate the reaction mechanism for the bromolactonization in the aprotic DCE solvent, using **1c** (Ar = *p*-Br–C_6H_4–) as the model substrate. Consistent with previous experimental and theoretical studies,[17,18] DFT calculations revealed that in DCE, the bromolactonization takes place *via* a *syn*-concerted addition pathway (Fig. 1). No transition state for the stepwise mechanism as well as *anti*-concerted addition pathway could be located. Interestingly, the activation barriers for the *syn*-additions are calculated to be fairly high, amounting to 36.8 and 39.4 kcal mol^{-1} for **TS-1** and **TS-2**, respectively. This DFT result is in good agreement with our experimental findings (Table 1) that only a trace

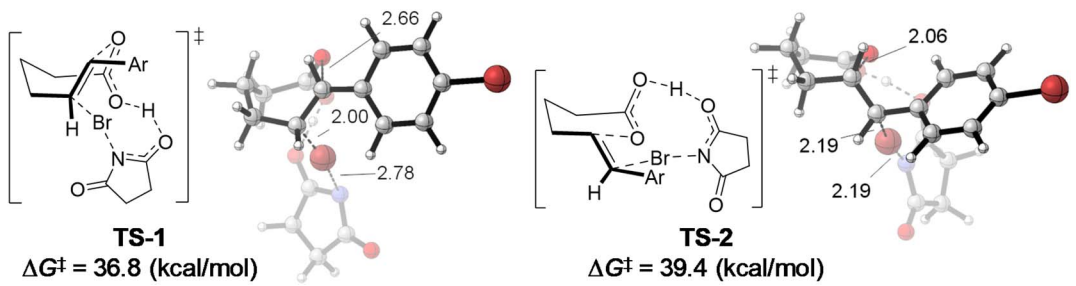

Fig. 1 Optimized transition states for the concerted bromolactonization in DCE. Transition states **TS-1** and **TS-2** lead to *endo*- and *exo*-cyclic products, respectively.

amount of the lactonization product can be observed when this reaction is performed in DCE (*vide supra*).

DFT calculations were subsequently performed to investigate the favorable mechanistic pathway and regioselectivity for the bromolactonization in HFIP. Because of its powerful hydrogen bond (H-bond) donor ability,[6a,d] it is possible for HFIP to form strong H-bonds with various species along the reaction course. Therefore, a mixed explicit–implicit solvation model is used, in

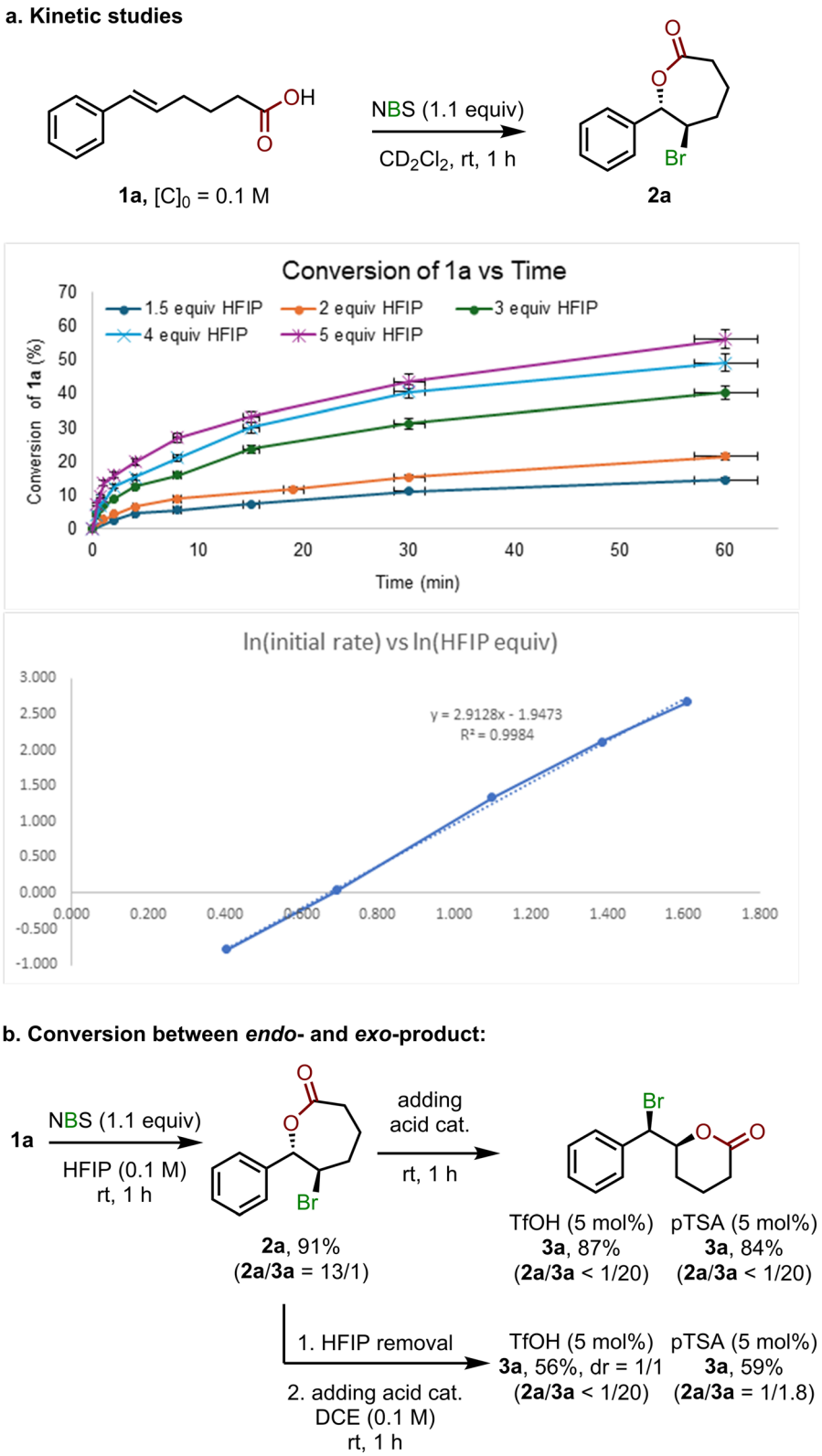

Fig. 2 Experimental mechanistic studies: (a) kinetics studies and (b) conversion between *endo*- and *exo*-product. See pages S6–S9 in the ESI† for more details.

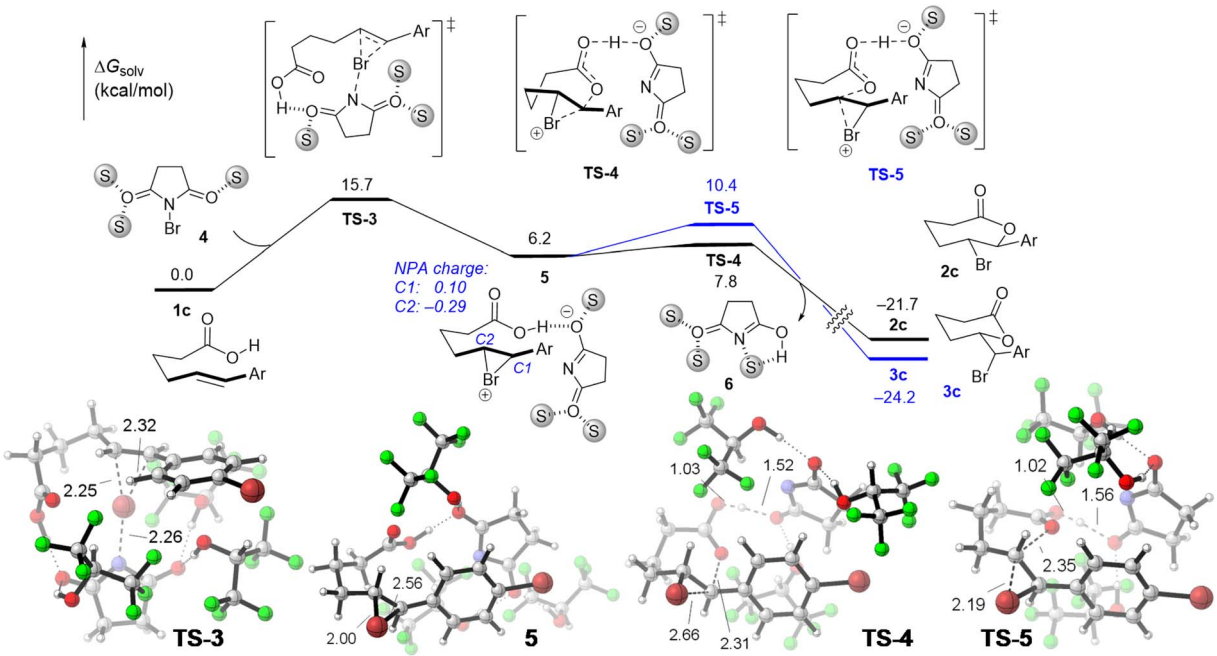

Fig. 3 Computed free energy profile for the stepwise bromolactonization in HFIP. S represents the HFIP molecule.

which explicit HFIP molecules were included in DFT calculations.[9,12b,19] Based on our kinetic studies suggesting that the reaction order in HFIP is approximately 3 (Fig. 2a and further details in pages S6–S8 in the ESI†), three HFIP molecules were included in our computational investigations. Additionally, we have also performed calculations by involving one and two HFIP molecules (Fig. S1–S4, pages S99–S100 in the ESI†). Although there are some changes in absolute energy values, the conclusion remains similar all through our calculations, which gives a solid validation to the accuracy of the mixed explicit–implicit solvation model.

Our DFT calculations indicated that the favorable mechanism for the bromolactonization in HFIP is the stepwise pathway (Fig. 3), which is consistent with the previous calculation for the

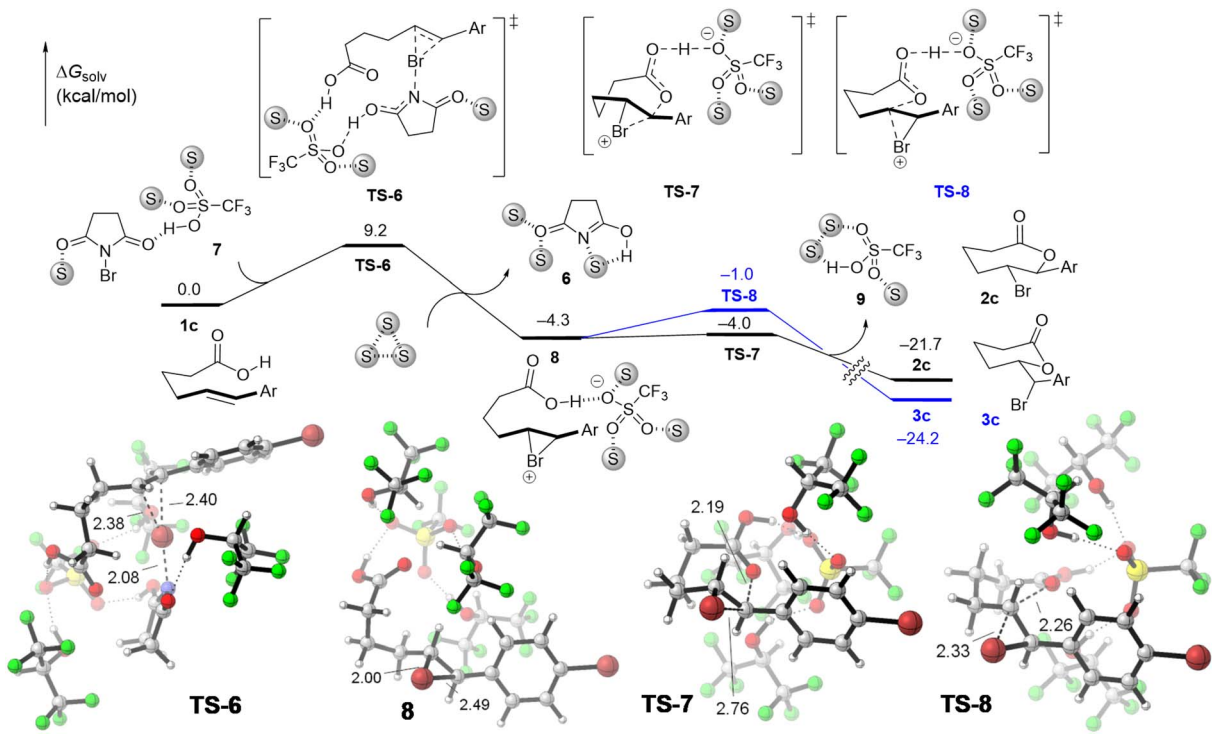

Fig. 4 Computed free energy profile for the stepwise bromolactonization in HFIP catalyzed by TfOH. S represents the HFIP molecule.

halolactonization in protic solvent.[18] The barrier height for the formation of the bridged bromonium species **5** *via* **TS-3** is calculated to be 15.7 kcal mol^{-1}. It should be noted that we have also considered the concerted mechanism for this transformation in HFIP. However, we can only locate the transition state for the *syn*-concerted addition pathway (Fig. S5 in the ESI†), which is calculated to be 9.7 kcal mol^{-1} higher in energy than **TS-3**. Therefore, the concerted mechanism is unlikely to occur. Additionally, the stepwise mechanism is also calculated to be the favorable pathway for the reaction of **1l** in HFIP (see Fig. S6 in the ESI† for more details). This result is in agreement with the fact that HFIP has an exceptional cation stabilization ability[6a,20] due to the low nucleophilicity and high dielectric constant, and, thus, the stepwise mechanism is supposed to be the preferable pathway.[16b]

In the bridged bromonium intermediate **5**, the natural charge of the C1 atom is higher than that of the C2 atom (Fig. 3). Therefore, the activation barrier for the nucleophilic addition from the oxygen atom of the carboxyl moiety to the C2 atom of the bromonium cation leading to the *endo*-cyclic product is calculated to be 2.6 kcal mol^{-1} lower in energy than that for the nucleophilic addition to the C1 atom. This result is consistent with experimental data where the formation of the *endo*-product is more favorable in HFIP. Our computational study demonstrates that the regioselectivity for the bromolactonization in HFIP is determined by electronic properties and this reaction is under kinetic control.

On the other hand, our experiments demonstrated that when TfOH is used as a catalyst, the *exo*-cyclic product is more favorable (Table 1). By using DFT calculations, we found that in the presence of TfOH, the NBS reagent can easily be protonated lowering the LUMO energy from −1.05 eV to −2.04 eV for neutral and protonated NBS, respectively leading to the enhancement of NBS reactivity.[21] When TfOH is included, the activation barrier for the electrophile addition **TS-6** is calculated to be 9.2 kcal mol^{-1} relative to **1** (Fig. 4), which is 6.5 kcal mol^{-1} lower than that without TfOH, *i.e.*, **TS-3**. In addition, TfOH can also have a great stabilization effect on the bridged bromonium species. From bromonium intermediate **8**, although the nucleophilic addition generating the *endo*-product is kinetically more favorable, the reaction is now under thermodynamic control. The *endo*-product can isomerize to generate a more stable *exo*-cyclic product. This computational result is consistent with our additional control experiments, in which the *endo*-cyclic species **2** can transform into the *exo*-cyclic species **3** in the presence of TfOH or pTSA (Fig. 2b – upper route, also see page S9 in the ESI† for more details). It should be noted that when the isomerization was carried out in DCE instead of HFIP (Fig. 2b – lower route), average yields of *exo*-product **3a** with poor diastereoselectivity (in the case of TfOH) or incomplete conversion (in the case of pTSA) were observed, highlighting the vital role of HFIP in this conversion.

Conclusion

In summary, we introduce an effective and straightforward method to access two different analogues of bromolactones by precisely manipulating the regioselectivity of the bromolactonization reaction in HFIP solvent. DFT calculations underscored the significance of HFIP in both *endo*-bromolactonization under kinetic conditions and *exo*-bromolactonization under thermodynamic conditions. This method, when combined with our recently developed ring-opening olefination of cyclic ketone ketals, offers a novel pathway for late-stage modifications of cyclic ketones into functionalized lactones.

Data availability

All data are available in the main text or the ESI.†

Author contributions

Conceptualization: TAT and TVN. Experimental work: NTAP and TAT. Computational work: BKM. Supervision: TVN. Writing – original draft: TAT, BKM, and TVN. Writing – review & editing: TVN.

Conflicts of interest

The authors declare that they have no competing interests.

Acknowledgements

Australian Research Council: FT180100260 (TVN) and DP200100063 (TVN). The authors thank the Australian Research Council and the UNSW Faculty of Science for financial support.

References

1 (*a*) G. H. Schmid, in *Double-Bonded Functional Groups*, 1989, pp. 679–731; (*b*) M.-F. Ruasse, in *Advances in Physical Organic Chemistry*, ed. D. Bethell, Academic Press, 1993, vol. 28, pp. 207–291; (*c*) A. Castellanos and S. P. Fletcher, Current Methods for Asymmetric Halogenation of Olefins, *Chem.–Eur. J.*, 2011, **17**, 5766–5776; (*d*) S. E. Denmark, W. E. Kuester and M. T. Burk, Catalytic, Asymmetric Halofunctionalization of Alkenes—A Critical Perspective, *Angew. Chem., Int. Ed.*, 2012, **51**, 10938–10953; (*e*) U. Hennecke, New Catalytic Approaches towards the Enantioselective Halogenation of Alkenes, *Chem.–Asian J.*, 2012, **7**, 456–465; (*f*) J. Chen and L. Zhou, Recent Progress in the Asymmetric Intermolecular Halogenation of Alkenes, *Synthesis*, 2014, **46**, 586–595; (*g*) Y. A. Cheng, W. Z. Yu and Y.-Y. Yeung, Recent advances in asymmetric intra- and intermolecular halofunctionalizations of alkenes, *Org. Biomol. Chem.*, 2014, **12**, 2333–2343; (*h*) A. J. Cresswell, S. T.-C. Eey and S. E. Denmark, Catalytic, Stereoselective Dihalogenation of Alkenes: Challenges and Opportunities, *Angew. Chem., Int. Ed.*, 2015, **54**, 15642–15682.

2 (*a*) S. A. Snyder, D. S. Treiler and A. P. Brucks, Halonium-Induced Cyclization Reactions, *Aldrichimica Acta*, 2011, **44**, 27–40; (*b*) A. Mendoza, F. J. Fananas and F. Rodríguez, Asymmetric Halocyclizations of Unsaturated Compounds:

An Overview and Recent Developments, *Curr. Org. Synth.*, 2013, **10**, 384–393; (*c*) S. Zheng, C. M. Schienebeck, W. Zhang, H.-Y. Wang and W. Tang, Cinchona Alkaloids as Organocatalysts in Enantioselective Halofunctionalization of Alkenes and Alkynes, *Asian J. Org. Chem.*, 2014, **3**, 366–376; (*d*) J. R. Wolstenhulme and V. Gouverneur, Asymmetric Fluorocyclizations of Alkenes, *Acc. Chem. Res.*, 2014, **47**, 3560–3570; (*e*) M. H. Gieuw, Z. Ke and Y.-Y. Yeung, Lewis Base Catalyzed Stereo- and Regioselective Bromocyclization, *Chem. Rec.*, 2017, **17**, 287–311; (*f*) B. Maji, Stereoselective Haliranium, Thiiranium and Seleniranium Ion-Triggered Friedel–Crafts-Type Alkylations for Polyene Cyclizations, *Adv. Synth. Catal.*, 2019, **361**, 3453–3489; (*g*) A. Maria Faisca Phillips and A. J. L. Pombeiro, Recent Developments in Enantioselective Organocatalytic Cascade Reactions for the Construction of Halogenated Ring Systems, *Eur. J. Org Chem.*, 2021, **2021**, 3938–3969; (*h*) J. Yan, Z. Zhou, Q. He, G. Chen, H. Wei and W. Xie, The applications of catalytic asymmetric halocyclization in natural product synthesis, *Org. Chem. Front.*, 2022, **9**, 499–516; (*i*) R. Nishiyori, T. Mori, K. Okuno and S. Shirakawa, Chiral sulfide and selenide catalysts for asymmetric halocyclizations and related reactions, *Org. Biomol. Chem.*, 2023, **21**, 3263–3275.

3 (*a*) M. D. Dowle and D. I. Davies, Synthesis and synthetic utility of halolactones, *Chem. Soc. Rev.*, 1979, **8**, 171–197; (*b*) Y. I. Gevaza and V. I. Staninets, Electrophilic heterocyclization of unsaturated carboxylic acids in the synthesis of lactones (review), *Chem. Heterocycl. Compd.*, 1988, **24**, 1073–1088; (*c*) M. Grabarczyk, K. Wińska and W. Mączka, An Overview of Synthetic Methods for the Preparation of Halolactones, *Curr. Org. Synth.*, 2019, **16**, 98–111; (*d*) W. Liu and N. Winssinger, Synthesis of α-exo-Methylene-γ-butyrolactones: Recent Developments and Applications in Natural Product Synthesis, *Synthesis*, 2021, **53**, 3977–3990.

4 (*a*) C. K. Tan, L. Zhou and Y.-Y. Yeung, Organocatalytic Enantioselective Halolactonizations: Strategies of Halogen Activation, *Synlett*, 2011, **2011**, 1335–1339; (*b*) J. M. J. Nolsøe and T. V. Hansen, Asymmetric Iodolactonization: An Evolutionary Account, *Eur. J. Org Chem.*, 2014, **2014**, 3051–3065; (*c*) R. Kristianslund, J. E. Tungen and T. V. Hansen, Catalytic enantioselective iodolactonization reactions, *Org. Biomol. Chem.*, 2019, **17**, 3079–3092.

5 J. D. Griffin, C. L. Cavanaugh and D. A. Nicewicz, Reversing the Regioselectivity of Halofunctionalization Reactions through Cooperative Photoredox and Copper Catalysis, *Angew. Chem., Int. Ed.*, 2017, **56**, 2097–2100.

6 (*a*) I. Colomer, A. E. R. Chamberlain, M. B. Haughey and T. J. Donohoe, Hexafluoroisopropanol as a highly versatile solvent, *Nat. Rev. Chem.*, 2017, **1**, 0088; (*b*) V. Pozhydaiev, M. Power, V. Gandon, J. Moran and D. Lebœuf, Exploiting hexafluoroisopropanol (HFIP) in Lewis and Brønsted acid-catalyzed reactions, *Chem. Commun.*, 2020, **56**, 11548–11564; (*c*) T. Bhattacharya, A. Ghosh and D. Maiti, Hexafluoroisopropanol: the magical solvent for Pd-catalyzed C–H activation, *Chem. Sci.*, 2021, **12**, 3857–3870; (*d*) H. F. Motiwala, A. M. Armaly, J. G. Cacioppo, T. C. Coombs, K. R. K. Koehn, V. M. I. V. Norwood and J. Aubé, HFIP in Organic Synthesis, *Chem. Rev.*, 2022, **122**, 12544–12747.

7 M. Piejko, J. Moran and D. Lebœuf, Difunctionalization Processes Enabled by Hexafluoroisopropanol, *ACS Org. Inorg. Au*, 2024, DOI: **10.1021/acsorginorgau.3c00067**.

8 (*a*) A. M. Arnold, A. Pöthig, M. Drees and T. Gulder, NXS, Morpholine, and HFIP: The Ideal Combination for Biomimetic Haliranium-Induced Polyene Cyclizations, *J. Am. Chem. Soc.*, 2018, **140**, 4344–4353; (*b*) J. Binder, A. Biswas and T. Gulder, Biomimetic chlorine-induced polyene cyclizations harnessing hypervalent chloroiodane–HFIP assemblies, *Chem. Sci.*, 2023, **14**, 3907–3912.

9 C. Qi, G. Force, V. Gandon and D. Lebœuf, Hexafluoroisopropanol-Promoted Haloamidation and Halolactonization of Unactivated Alkenes, *Angew. Chem., Int. Ed.*, 2021, **60**, 946–953.

10 M. A. Hussein, U. P. N. Tran, V. T. Huynh, J. Ho, M. Bhadbhade, H. Mayr and T. V. Nguyen, Halide Anion Triggered Reactions of Michael Acceptors with Tropylium Ion, *Angew. Chem., Int. Ed.*, 2020, **59**, 1455–1459.

11 (*a*) U. P. N. Tran, G. Oss, D. P. Pace, J. Ho and T. V. Nguyen, Tropylium-promoted carbonyl–olefin metathesis reactions, *Chem. Sci.*, 2018, **9**, 5145–5151; (*b*) G. Oss and T. V. Nguyen, Iodonium-Catalyzed Carbonyl–Olefin Metathesis Reactions, *Synlett*, 2019, **30**, 1966–1970; (*c*) U. P. N. Tran, G. Oss, M. Breugst, E. Detmar, D. P. Pace, K. Liyanto and T. V. Nguyen, Carbonyl–Olefin Metathesis Catalyzed by Molecular Iodine, *ACS Catal.*, 2019, **9**, 912–919; (*d*) K. Omoregbee, K. N. H. Luc, A. H. Dinh and T. V. Nguyen, Tropylium-promoted prenylation reactions of phenols in continuous flow, *J. Flow Chem.*, 2020, **10**, 161–166; (*e*) D. P. Pace, R. Robidas, U. P. N. Tran, C. Y. Legault and T. V. Nguyen, Iodine-Catalyzed Synthesis of Substituted Furans and Pyrans: Reaction Scope and Mechanistic Insights, *J. Org. Chem.*, 2021, **86**, 8154–8171; (*f*) J. S. Mann, B. K. Mai and T. V. Nguyen, Carbocation-Catalyzed Intramolecular and Intermolecular Carbonyl-Alkyne Metathesis Reactions, *ACS Catal.*, 2023, **13**, 2696–2701; (*g*) B. Pu and T. V. Nguyen, HFIP-assisted Brønsted acid catalysed synthesis of furan derivatives, *Aust. J. Chem.*, 2023, **76**, 58–62.

12 (*a*) M. A. Hussein, A. H. Dinh, V. T. Huynh and T. V. Nguyen, Synthesis of tertiary amines by direct Brønsted acid catalyzed reductive amination, *Chem. Commun.*, 2020, **56**, 8691–8694; (*b*) T. A. To, C. Pei, R. M. Koenigs and T. V. Nguyen, Hydrogen Bonding Networks Enable Brønsted Acid-Catalyzed Carbonyl-Olefin Metathesis, *Angew. Chem., Int. Ed.*, 2022, **61**, e202117366; (*c*) T. A. To, B. K. Mai and T. V. Nguyen, Toward Homogeneous Brønsted-Acid-Catalyzed Intramolecular Carbonyl–Olefin Metathesis Reactions, *Org. Lett.*, 2022, **24**, 7237–7241.

13 T. A. To and T. V. Nguyen, Olefination of Aromatic Carbonyls via Site-Specific Activation of Cycloalkanone Ketals, *Angew. Chem., Int. Ed.*, 2024, **63**, e202317003.

14 R.-J. Tang, T. Milcent and B. Crousse, Regioselective Halogenation of Arenes and Heterocycles in Hexafluoroisopropanol, *J. Org. Chem.*, 2018, **83**, 930–938.

15 W. Wang, X. Yang, R. Dai, Z. Yan, J. Wei, X. Dou, X. Qiu, H. Zhang, C. Wang, Y. Liu, S. Song and N. Jiao, Catalytic Electrophilic Halogenation of Arenes with Electron-Withdrawing Substituents, *J. Am. Chem. Soc.*, 2022, **144**, 13415–13425.

16 (*a*) I. Roberts and G. E. Kimball, The Halogenation of Ethylenes, *J. Am. Chem. Soc.*, 1937, **59**, 947–948; (*b*) G. A. Olah and J. M. Bollinger, Stable carbonium ions. XLVIII. Halonium ion formation via neighboring halogen participation. Tetramethylethylene halonium ions, *J. Am. Chem. Soc.*, 1967, **89**, 4744–4752.

17 (*a*) K. D. Ashtekar, M. Vetticatt, R. Yousefi, J. E. Jackson and B. Borhan, Nucleophile-Assisted Alkene Activation: Olefins Alone Are Often Incompetent, *J. Am. Chem. Soc.*, 2016, **138**, 8114–8119; (*b*) N. Salehi Marzijarani, R. Yousefi, A. Jaganathan, K. D. Ashtekar, J. E. Jackson and B. Borhan, Absolute and relative facial selectivities in organocatalytic asymmetric chlorocyclization reactions, *Chem. Sci.*, 2018, **9**, 2898–2908; (*c*) R. Yousefi, A. Sarkar, K. D. Ashtekar, D. C. Whitehead, T. Kakeshpour, D. Holmes, P. Reed, J. E. Jackson and B. Borhan, Mechanistic Insights into the Origin of Stereoselectivity in an Asymmetric Chlorolactonization Catalyzed by $(DHQD)_2PHAL$, *J. Am. Chem. Soc.*, 2020, **142**, 7179–7189.

18 R. Van Lommel, J. Bock, C. G. Daniliuc, U. Hennecke and F. De Proft, A dynamic picture of the halolactonization reaction through a combination of *ab initio* metadynamics and experimental investigations, *Chem. Sci.*, 2021, **12**, 7746–7757.

19 (*a*) S. Bag, S. K, A. Mondal, R. Jayarajan, U. Dutta, S. Porey, R. B. Sunoj and D. Maiti, Palladium-Catalyzed *meta*-C–H Allylation of Arenes: A Unique Combination of a Pyrimidine-Based Template and Hexafluoroisopropanol, *J. Am. Chem. Soc.*, 2020, **142**, 12453–12466; (*b*) Y. Zhou, R.-C. Xue, Y. Feng and L. Zhang, How Does HOTf/HFIP Cooperative System Catalyze the Ring-Opening Reaction of Cyclopropanes? A DFT Study, *Asian J. Org. Chem.*, 2020, **9**, 311–316.

20 A. M. Arnold, P. Dullinger, A. Biswas, C. Jandl, D. Horinek and T. Gulder, Enzyme-like polyene cyclizations catalyzed by dynamic, self-assembled, supramolecular fluoro alcohol-amine clusters, *Nat. Commun.*, 2023, **14**, 813.

21 D. Barišić, I. Halasz, A. Bjelopetrović, D. Babić and M. Ćurić, Mechanistic Study of the Mechanochemical Pd^{II}-Catalyzed Bromination of Aromatic C–H Bonds by Experimental and Computational Methods, *Organometallics*, 2022, **41**, 1284–1294.